Measurement of CO_2 in Outdoor Environments Using LPWAN Based WSN and Its Time Correlation Characteristics

Koki Kitazumi*, Ryoma Yasutani*, Shusuke Narieda† and Hiroshi Naruse†
* Dept. Eng., Mie Univ., Japan.
† Graduate School of Eng., Mie Univ., Mie, Japan.
E-mail: narieda@pa.info.mie-u.ac.jp†

***Abstract*—In this paper, we discuss time correlation characteristics for measurement results of carbon dioxide (CO_2) concentration in outdoor environments. The purpose of this paper is to collect an information for the effective placement of sensor nodes in wireless sensor networks (WSNs). We observed CO_2 concentration using WSNs based on low-power wide area networks (LPWANs). To measure CO_2 concentration in outdoor environments, some sensor nodes with CO_2 sensor are deployed in Kamihama campus, Mie University, Japan, and CO_2 concentration on the area are measured using LPWAN based WSN. We provide the time correlation characteristics based on the measurement results, and the time correlation characteristics of CO_2 concentration are compared with that of relative humidity.**

I. Introduction

Emerging of the Internet of Things (IoT) technologies provides the possibility of centralized data accessibility and data fusion. A lot of IoT devices are deployed everywhere to gather information for physical quantities, and it is possible to construct a wireless sensor network (WSN) of unprecedented scale. In general, the WSNs have one gateway and a lot of sensor nodes with characteristics such as low-cost, low-power driven and multi-functional. The WSNs can be also realized by employing low power wide area (LPWA) communication technologies [1] having the capabilities of long range communications and battery efficiencies, and these features are suitable for the construction of the WSN. Among a lot of LPWA technologies, Long Range (LoRa) communications [2] can easily develop such a WSN system because the LoRa networks can be used to construct a private/local network in an unlicensed band.

On the other hand, several applications based on WSN with LPWA technologies have been analyzed; for a smart golf course [3], smart city application [3], [4], and environmental monitoring [5], [6], [7]. Among them, environmental monitoring is a broad area focusing on using scientific and engineering principles for the improvement of environmental condition. Environmental informatics, which is an interdisciplinary field involving computer science, information science and environmental science, has a very rapidly developed, and it enables to provide a solution for specific environmental problems related to the computer science. The rapid development of environmental informatics has significantly improved environmental monitoring. Especially, for the recent COVID-19 pandemic, it is necessary for the monitoring of carbon dioxide (CO_2) concentration, and it can be said that the importance of the environmental monitoring is increasing.

It is important to construct and design of the WSN for the specific purpose in order to achieve the best performance at a limited cost. Especially, it is important the placement of sensor nodes in the WSN because it has a large effect on the cost and measurement accuracy. Traditionally, many researches have focused on a hardware for environmental monitoring [7], [8], [9] whereas the constructions of WSN for environmental monitoring, e.g., placement of the sensor nodes, have never been focused. To pursuit the purpose, we have investigated the relationship between the geographical location and the behavior of time change in measured physical quantity, i.e., temperature, relative humidity and atmospheric pressure [10]. In this paper, we provide the investigation results of the time correlation characteristics of CO_2 concentration in outdoor environment.

II. Analytics Method of Measured Physical Quantities

In this section, we show analytics method of measured physical quantities. The analyses in this paper are based on some statistics to evaluate the geographical and temporal relationship between each measured physical quantity, and the relationship will be available for the optimization of the sensor node placement. To investigate the geographical and temporal relationship, we employ the cross correlation coefficient and the average relative error between each measured quantity. In the experiment, the measurements are executed at some geographically different points where the sensor node is located, and some of these points are used for the computation of the cross correlation coefficient and the relative error as a reference point. We let $x_i(n)$, $x_{\text{REF},k}(n)$, $\overline{x_i}$ and $\overline{x_{\text{REF},k}}$ denote an ith measured quantity at n, a measured quantity at n on the kth reference point, an average of $x(n)$ and an average of $x_{\text{REF},k}(n)$, respectively. Then, the cross correlation coefficient $\overline{C_{x_i,x_{\text{REF},k}}}(\tau)$ between the measured quantity $x_i(n)$ at the ith sensor node and the measured quantity $x_{\text{REF},k}(n)$ at the kth reference point is given by

$$\overline{C_{x_i,x_{\text{REF},k}}}(\tau) = \frac{1}{N}\sum_{n=0}^{N-1}\frac{\{x_i(n)-\overline{x_i}\}\{x_{\text{REF},k}(n+\tau)-\overline{x_{\text{REF},k}}\}}{\sqrt{C_{x_i,x_i}(0)C_{x_{\text{REF},k},x_{\text{REF},k}}(0)}}, \tag{1}$$

where τ, N, $C_{x_i,x_i}(\tau)$ and $C_{x_{\text{REF},k},x_{\text{REF},k}}(\tau)$ are a time delay, the number of samples for $x(n)$ and $x_{\text{REF},k}(n)$, an autocorrelation function of $x(n)$ and an autocorrelation function of $x_{\text{REF},k}(n)$, respectively. Further, the average relative error $\overline{\epsilon_{i,k}}$ between the ith measured quantity and the kth reference point is given by

$$\overline{\epsilon_{i,k}} = \frac{1}{N}\sum_{n=0}^{N-1}\left|\frac{x_i(n)-x_{\text{REF},k}(n)}{x_{\text{REF},k}(n)}\right|. \tag{2}$$

Based on $\overline{C_{x_i,x_{\text{REF},k}}}(\tau)$ and $\overline{\epsilon_{i,k}}$, the geographical and temporal relationship of the measured physical quantities for the WSN based environmental monitoring. $\overline{C_{x_i,x_{\text{REF},k}}}(\tau)$ close to 1 means that there is almost no difference in the behavior of changes in the two measured quantities. $\overline{\epsilon_{i,k}}$ close to 0 means that the two measured quantities are almost the same.

III. Measurement Setup

A. Measurement System

We employ the WSN based measurement systems which are consisted of one LoRa gateway and some sensor nodes. All sensor nodes observe the physical quantities and send them to the gateway, and to execute this, both the gateway and all the sensor nodes equip with the LoRa module. The LoRa gateway is composed of the LoRa module, receive antenna, Raspberry PI 3 B+ and battery with a capacity of $20,000$ mAh, as shown in Fig. 1(a). The LoRa module, which includes Semtech SX1276 [11] made by Semtech Inc., is manufactured by EASEL Inc. [12]. These equipment are housed in one Styrofoam box and the box is installed using a tripod as shown in Fig. 1(b).

The sensor node is composed of the LoRa module, receive antenna, Raspberry PI 3 B+, physical sensors, prototyping board and battery as shown in Fig. 2. Raspberry PI 3 B+ [13] is used for the control of physical sensors and the LoRa module. The LoRa module and some physical sensors are controlled by our developed system programmed by Python [14] which is a programming language for general purposes. The sensor node has two types of physical sensors which are for the measurements of CO_2 concentration and relative humidity. Note that the measurement of relative humidity is executed to compare with the time correlation characteristics of CO_2 concentration. These sensors are connected to Raspberry PI 3 B+ via the prototyping board. These equipment are also housed in one Styrofoam box, and it is similar to it placed on tripod in Fig. 1(b).

B. Measurement Scheme

In the experiments, the sensor nodes shown in previous subsection are placed in the measurement area and they measure CO_2 concentration and relative humidity at each located position. Fig. 3 shows a measurement area for the experiments of the environmental monitoring system which is the part of the Kamihama campus of Mie University, Japan, having a land area of approximately $350\,\text{m} \times 280\,\text{m}$. We have confirmed that another LPWA technologies operating 920 MHz frequency bands are not activated in the area including neighboring. The LoRa gateway is placed at the yellow star in the center of Fig. 3, and it is placed on the rooftop of a five-stories reinforced concrete building, approximately 19.4 m in height. The sensor nodes are placed at white small circles with number in Fig. 3. The number of the circles is 30 including 26 white circles and 4 black circles. The black circles with the number mean a reference point to compute the cross correlation coefficient and the average relative error.

To compute these statistics at gateway, the measured physical quantities at each sensor node are sent to the gateway by LoRa communications with 922 MHz center frequency, 125 kHz signal bandwidth and 10 spreading factor. Each sensor node transmits each measured quantities to gateway once a hour, and then, the sending timing at each sensor node is offset by 20 seconds to avoid packet collision among each sensor node. In Japan, the unlicensed LPWA communications operate in the 920 MHz bands, and the Japanese regulations [15] for the unlicensed LPWA communications can be divided into two categories in which the maximum transmission power are 20 mW and 1 mW. In the 20 mW case, a carrier sense is required whereas it is not required in the 1 mW case. The

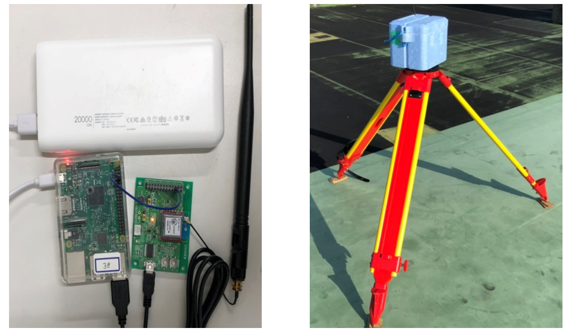

(a) Configuration of gateway (b) Overview of installation of gateway

Fig. 1. LoRa gateway

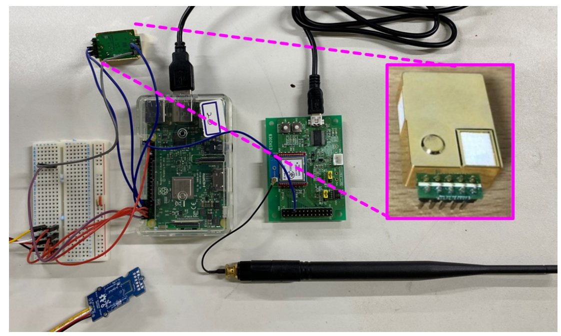

Fig. 2. Configuration of sensor node

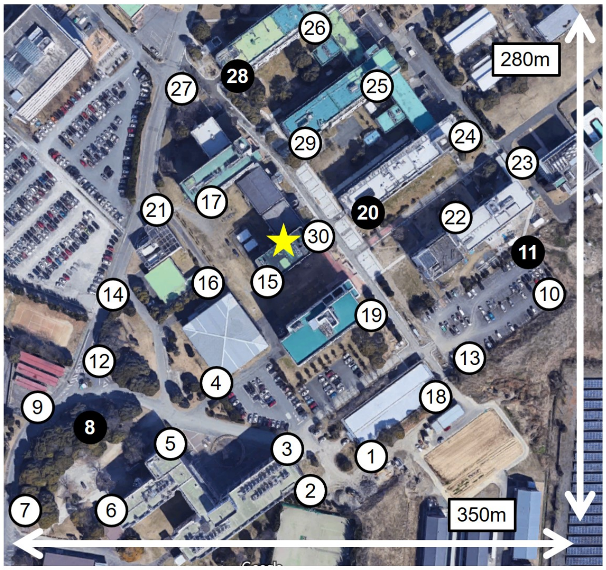

Fig. 3. Measurement area in experimental analysis.

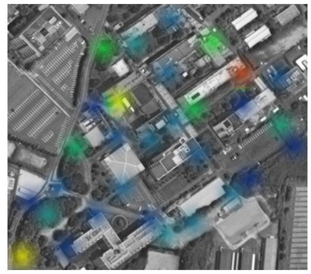

(a) result at 16:00 Jan. 6, 2021

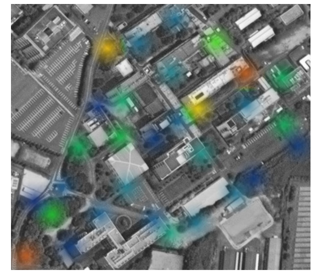

(b) result at 22:00 Jan. 6, 2021

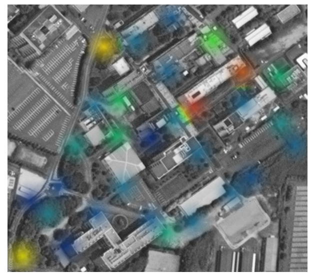

(c) result at 04:00 Jan. 7, 2021

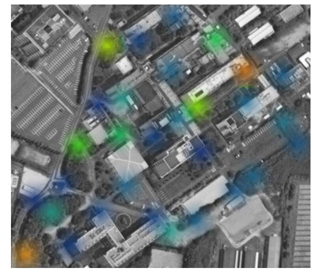

(d) result at 10:00 Jan. 7, 2021

(e) Color map for all results

Fig. 4. Measurement results of CO_2 concentration in measurement area and its behavior of time change in measurement results.

carrier sense is important in the unlicensed band because the LPWA can construct the private/local networks in Japan and some communication areas may overlap with each other. Furthermore, in the 20 mW case, a duty cycle is not specified and the transmission time at one time is specified (4 sec). Therefore, we employ the case of maximum transmission power is 20 mW in this paper.

IV. Experimental Analyses

The measurement results shown in this section were obtained via the experiments conducted from 15:00 on January 6, 2021 to 15:00 the following day. First, we show the measurement results of CO_2 concentration in Fig. 4. Although the raw data obtained by the measurement is shown as it is in Fig. 4, it is difficult to understand the behavior of time change in these measurement results. To understand the behavior, first, Table. I shows the cross correlation coefficient between the reference points and each measurement points. Each value in Table. I is the average of the cross correlation coefficients between each reference point and each ED. As

TABLE I
Average Cross Correlation Coefficient ($\tau = 0$)

	Ref. 8	Ref. 11	Ref. 20	Ref. 28
CO_2	0.30	0.35	0.27	0.14
RH	0.93	0.91	0.93	0.94

shown in Table. I, it can be seen that low average cross correlation coefficient can be obtained for the measured CO_2 concentration whereas the high average cross correlation coefficient can be obtained for the measured relative humidity. To show details of the relationship between the cross correlation coefficient and geographical location, Fig. 5 shows geographically plots of the cross correlation coefficient for each reference point. From Fig. 5, it can be also seen that the measured CO_2 concentration has a lower cross correlation coefficient than the measured relative humidity regardless of the measurement location. Finally, we show the relationship between the cross correlation coefficient and the relative error of the measurement physical quantities. Fig. 6 shows the relationship for all the measured quantities at all the reference points. As shown in Fig. 6, the measured relative humidity have a high cross correlation coefficient and a small relative error, and this means that a similar measured quantity can be obtained within the measurement area as shown in Fig. 3, and it can be seen that the measurement of relative humidity does not require a lot of sensor nodes. On the other hand, the measured CO_2 concentration has a large relative error and a large variation of the cross correlation coefficient. This means that similar measured CO_2 concentration is not obtained within the measurement area, and it can be seen that the measurement of CO_2 concentration requires a lot of sensor nodes to grasp the behavior of time change accurately.

V. Conclusion

This paper discussed the time correlation characteristics of CO_2 concentration based on the measurement results in outdoor environments. The purpose of this paper was to collect an information for the effective placement of sensor nodes in the WSNs. The measurements of CO_2 concentration and relative humidity are executed using LPWAN based WSN

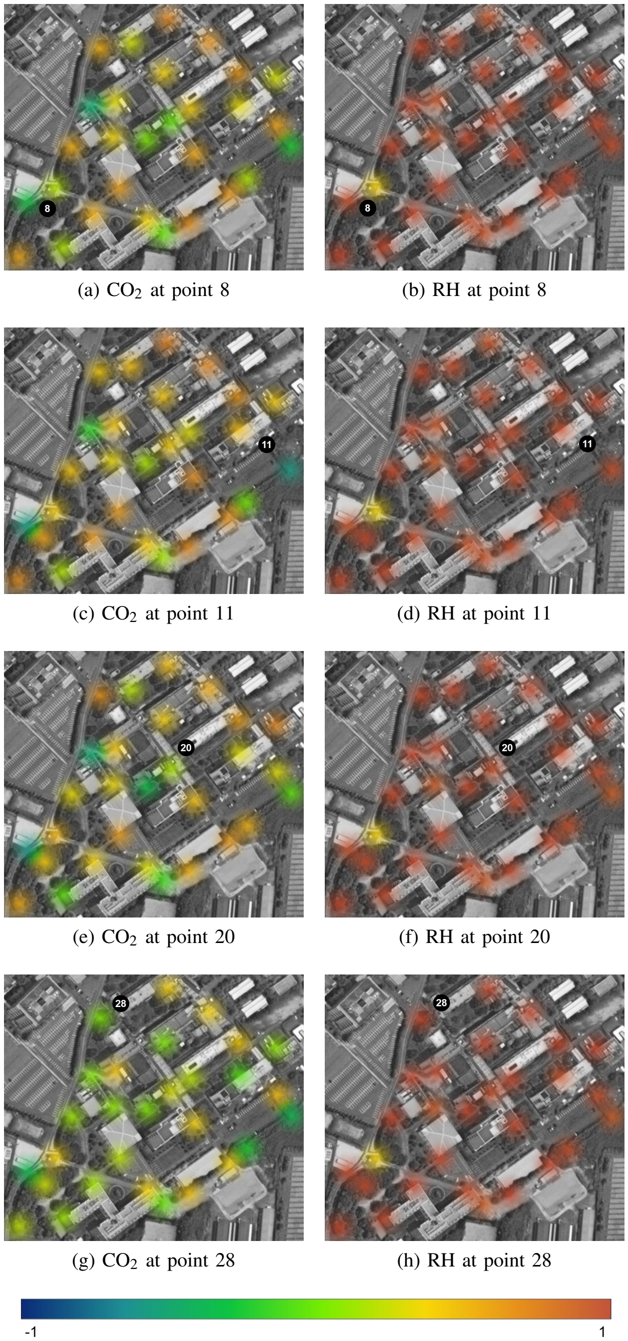

(a) CO_2 at point 8 (b) RH at point 8

(c) CO_2 at point 11 (d) RH at point 11

(e) CO_2 at point 20 (f) RH at point 20

(g) CO_2 at point 28 (h) RH at point 28

(i) Color map for all results

Fig. 5. Cross correlation coefficient plotted on measurement area for each measured physical quantities at each reference point.

in Kamihama campus, Mie University, Japan. We provided the time correlation characteristics based on the measurement results. Analysis results showed that the cross correlation coefficient of CO_2 concentration between each sensor node is much smaller than that of relative humidity.

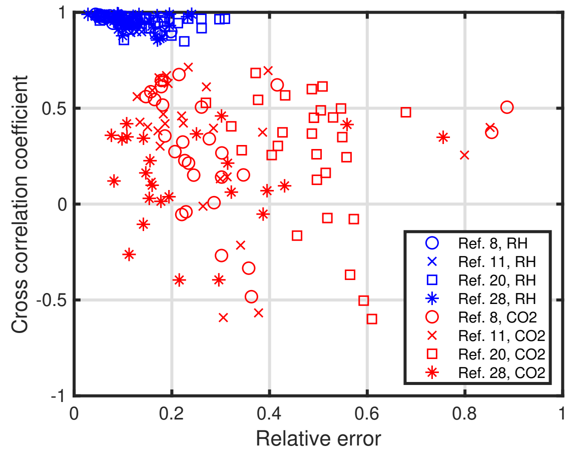

Fig. 6. Relationship between cross correlation coefficient and relative error for all reference point.

ACKNOWLEDGMENT

This research and development work was supported by JSPS KAKENHI Grant Number JP19K04374.

REFERENCES

[1] U. Raza, P. Kulkami, and M. Sooriyabandara, "Low Power Wide Area Networks: An Overview," *IEEE Commun. Surveys Tuts.*, vol. 19, no. 2, pp. 855–873, Secondquater 2017.
[2] https://lora-alliance.org/.
[3] J. P. Shanmuga Sundaram, W. Du, and Z. Zhao, "A Survey on LoRa Networking: Research Problems, Current Solutions, and Open Issues," *IEEE Communications Surveys and Tutorials*, vol. 22, no. 1, pp. 371–388, 2020.
[4] D. Magrin, M. Centenaro, and L. Vangelista, "Performance Evaluation of LoRa Networks in A Smart City Scenario," in *Proceeding of the 2017 IEEE International Conference on Communications (ICC)*, 2017, pp. 1–6.
[5] L. Joris, F. Dupont, P. Laurent, P. Bellier, S. Stoukatch, and J. Redoute, "An Autonomous Sigfox Wireless Sensor Node for Environmental Monitoring," *IEEE Sensors Letters*, vol. 3, no. 7, pp. 01–04, 2019.
[6] J. Botero-valencia, L. Castano-Londono, D. Marquez-Viloria, and M. Rico-Garcia, "Data Reduction in a Low-Cost Environmental Monitoring System Based on LoRa for WSN," *IEEE Internet of Things Journal*, vol. 6, no. 2, pp. 3024–3030, 2019.
[7] M. T. Lazarescu, "Design of a WSN Platform for Long-Term Environmental Monitoring for IoT Applications," *IEEE Journal on Emerging and Selected Topics in Circuits and Systems*, vol. 3, no. 1, pp. 45–54, 2013.
[8] L. Baumgartner, A. Penning, P. Lampe, B. Richerzhagen, R. Steinmetz, and B. Freisleben, "Environmental Monitoring Using Low-Cost Hardware and Infrastructureless Wireless Communication," in *2018 IEEE Global Humanitarian Technology Conference (GHTC)*, 2018, pp. 1–8.
[9] M. Haghi, S. Neubert, A. Geissler, H. Fleischer, N. Stoll, R. Stoll, and K. Thurow, "A Flexible and Pervasive IoT-Based Healthcare Platform for Physiological and Environmental Parameters Monitoring," *IEEE Internet of Things Journal*, vol. 7, no. 6, pp. 5628–5647, 2020.
[10] A. Kaichi, S. Narieda, T. Fujii, K. Umebayashi, and H. Naruse, "On Placement of End Devices in LPWAN based WSNfor Environmental Monitoring Applications," in *13th Asia Pacific Signal and Information Processing Association Annual Summit and Conference (APSIPA ASC)*, 2020, pp. 1–4.
[11] https://www.semtech.com/products/wireless-rf/lora-transceivers/sx1276.
[12] https://easel5.com/ (*in Japanese*).
[13] https://www.raspberrypi.org/.
[14] https://www.python.org/.
[15] ARIB STD-T108, v. 1.2, Jan. 2018. (*in Japanese*).